Bull. Jpn. Soc. Fish. Oceanogr. 68(2) 71–86, 2004

Development of PISCES – A User-friendly Software for PC to Produce Sea Surface Temperature Maps from High Resolution Satellite Data around Japan

Yoshihiro OKADA[†1,3], Makoto MORIWAKI[2] and Kedarnath MAHAPATRA[3]

To provide user-friendly daily sea surface temperature (SST) maps from high resolution satellite imagery of the Advanced Very High Resolution Radiometer (AVHRR) onboard the National Oceanic and Atmospheric Administration (NOAA) series of satellites in seas around Japan, we developed the PISCES—**P**C-based **I**maging **S**oftware for **C**ontinuous **E**stimation of **S**ST. The software system is aimed at achieving judicious removal of spurious cloudy pixels; oceanographically and statistically sound interpolation of SST for the cloud covered pixels and continuous regeneration of daily SST maps through a computerized automatic process. In this paper, we describe the configuration of the PISCES along with the statistical algorithms used to achieve various components of the software. The PISCES-interpolated SST output from the software for a sample day was validated against the real SST field for the same day, and both values were in good agreement (R^2=0.999). The PISCES-generated sample images for two selected areas near the Sanriku Coast and the Boso East Coast are presented in this paper as case studies, to demonstrate utility of the software to deal with the pattern of mesoscale as well as localized ocean surface thermal features. Despite limitation in tracing transient features such as undulations and eddies in the coastal oceans, the products were found to be useful in depicting major mesoscale features, and could meet the requirements of various potential users, mainly in the field of marine fisheries.

Key words: PC-software, AVHRR/NOAA, SST interpolation, SST maps, fisheries application

Introduction

In contrast to localized measurement of Sea Surface Temperature (SST) from ship and buoy, high spatial resolution thermal infrared (IR) images from the Earth-orbiting satellite offer an opportunity to generate SST maps for wide range of applications. Because of uninterrupted and wide availability of SST imagery from the Advanced Very High Resolution Radiometer (AVHRR) aboard the National Oceanic and Atmospheric Administration (NOAA) series of polar orbiting satellites during last two decades, such data are being widely used for various applications besides routine use in climatologic and oceanographic investigations. Detection of potential fishing ground for major pelagic species based on satellite derived SST has been operational in many maritime countries around the World. Forecast products containing such information are being generated by government and quasi-government agencies as well as private sectors. Some other potential area of application of SST products, are shipping and marine pollution detection such as thermal effluent from large power stations.

Satellite-derived SST field has been recognized as an important tool in delineation of pelagic fishing ground (Montgomery, 1981; Gower, 1982; Yamanaka, 1982; Laurs and Brucks, 1985; Fiedler *et al.*, 1985; Fiúza, 1990). Movement of ocean thermal features such as warm-core rings and streamers as detected from SST images, were found to play an important role in formation of pelagic fishing grounds in waters around Japan (Hirai, 1985; Saitoh *et al.*, 1986; Sugimoto and Tameishi, 1992). The Japan Fisheries Information Service Center (JAFIC) provides fishing ground forecast charts for the seas around Japan to the fishing vessels on operational basis. Such forecasts are produced using satellite derived SST in conjunction with fisheries oceanographic data collected in coordination with the fishing vessels. Localized SST charts has potential to be of use to the Japanese fishing community for enabling them to sustain the fishing operation by saving fuel and time seeking out areas of high productivity. This appears more relevant considering gradual decline in the number of people engaged in fishing operation in the recent years and increase in greying population in Japan. Satellite derived SST chart can also be a valuable supplementary input in shipping forecast to aid in decision making about engine cool-

Received April 14, 2003; Accepted October 10, 2003.

[1] School of Marine Science and Technology, TOKAI University, 3–20–1 Orido, Shimizu, Shizuoka 424–8610, Japan

[2] Earth Weather INC., 1–2–20 Nakamachidai, Tsuzuki-ku, Yokohama 224–0041, Japan

[3] Tokai University Frontier Ocean Research Center (T-FORCE), TOKAI University, 3–20–1 Orido, Shimizu, Shizuoka 424–8610, Japan

[†] okada@scc.u-tokai.ac.jp

ing operation of large cargo ships especially during the long voyage, as the sea water is used for cooling the engine systems of the ships. In view of the above potential utilities of SST and importance attached by the Japanese government to increased use of Internet for community development, there is immense scope for producing localized and user-friendly SST products using preferably PC-based software which can be accessed by the users as color coded maps from the web pages.

Clouds are considered to be the major limitations in generating the satellite-derived images regularly, as they obstruct sea-surface thermal IR radiation from reaching the satellite sensor. Since cloud-cover over a specific area is subjected to temporal changes and satellite covers all areas of the Earth surface, it is possible to produce "cloud-free" SST images through construction of composites and averaging techniques for the desired duration using repeat satellite images. Usually SST composites and averaged images are generated using images spanning over a couple of days to weeks through replacement of the gappy pixels under cloud cover by respectively the maximum and mean (or median) of the corresponding pixel values from a series of images. Such images are found to be useful for retrieval of the major ocean features even though they are of limited use in investigation of localized eddies or undulations in the ocean (Sakaida *et al.*, 2000). Furthermore, composite or averaged satellite images provide wide spatial coverage on a fairly short time scale compared with the charts based on ship SST observations. The cloud-free SST images are also regenerated by estimation of the SST at the gappy pixels through various interpolation techniques based on the spatial and temporal proximity of those pixels to the cloud-free pixels on a daily image. But on a daily image with extensive cloud cover such interpolation technique becomes difficult to implement. In such cases the cloudy areas can be filled up by transferring the cloud free pixels of the corresponding location from the image of the previous day or a composite for the preceding period, to reduce the cloud covered areas on an image. Such interpolation technique is expected to affect the accuracy of the SST charts. Hence it is necessary to improve accuracy with such technique before using for routine production of SST charts. It is worth noting that the SST charts based on interpolated satellite images are based on reasonably less cartographic and statistical manipulation compared to the SST charts prepared manually based on ship observations carried out at discrete stations spreading over a huge area over a period of a few days. However, manually interpreted SST charts are based on long experience of the personnel with the local oceanographic pattern in a given area. By incorporating the logic behind manual plotting of conventional SST charts into the computer based SST image processing software, it is possible to regenerate SST field over a cloud covered area and produce SST maps with the spatial resolution available from satellite data, based on judicious oceanographic inputs usually go into a manually plotted SST chart.

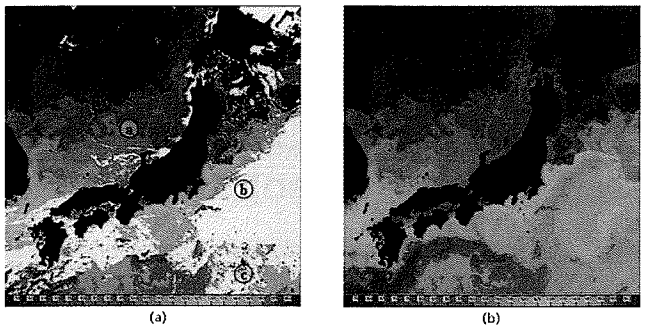

Figure 1. Sample input (a) and output (b) NOAA-AVHRR derived SST images covering ocean areas around Japan on February 22 2001. The output image is regenerated after removal of non-SST spurious pixels and interpolation of SST values at the cloudy pixels using the default functions of the PISCES. The encircled a, b, and c marked on the input image shows SST field, cloud-masked area, and the area with spurious pixels respectively.

Against the background as described above, we developed the PISCES* (**P**C-based **I**maging **S**oftware for **C**ontinuous **E**stimation of **S**ST) under a collaborative project of the Tokai University and the Earth Weather INC. The objective of this software is to generate SST maps from NOAA-AVHRR High Resolution Picture Transmission (HRPT) images with an image size of 512×512 pixels, covering the ocean areas surrounding Japan from 29.5°N to 44.7°N and 128°E to147°E with a grid size of 0.03 degree or 3.3 km. This ocean area is shown in Fig. 1. To achieve the localized coverage around Japan, the SST images can also be processed for specified areas from both coastal and oceanic waters surrounding Japan with varying grid sizes. The system is aimed at achieving the judicious removal of spurious cloudy pixels; oceanographically sound interpolation of SST for the cloud covered pixels and finally continuous regeneration of daily SST maps through computerized automatic process. A sample daily SST image used as input in the system and the regenerated image produced as the final output are presented in Fig. 1. In this paper we describe the characteristics of the PISCES system along with

* We coined the abbreviated name of the software, PISCES considering the association of the term with the sign of the ZODIAC represented by two fish and potential applicability of the software in marine fishery sector. The abbreviation PISCES is being used elsewhere for ocean models, *i.e.* Pelagic Interaction Scheme for Carbon and Ecosystem Studies, protocols, i.e. Protocols for Integrated Ship Control and Evaluation of Situation and laboratory, *i.e.* Paleoenvironmental Integrated Studies of Climate and Ecosystems *etc.*

the statistical algorithms used in various functions of the software. Effectiveness of the algorithms was further validated using the real time SST and the PISCES-regenerated SST from the sample images. Finally the output images of two sample areas generated from the PISCES are presented along with the thermal contour maps generated using ship data to underline the utility of such images in providing sea surface thermal field in general and some fishery oriented important ocean features in particular.

System characteristics of the PISCES

Direct broadcast reception and processing systems are being used to receive, process, display and archive HRPT data from NOAA-AVHRR. These systems use in-flight calibration to obtain the absolute brightness temperature and apply the Multi-channel SST (MCSST) algorithm (McClain *et al.*, 1985) or nonlinear SST (NLSST) algorithm (Walton, 1988; Walton *et al.*, 1998) on thermal bands of AVHRR to retrieve the SST from the brightness temperature. The coefficients for the MCSST algorithm and NLSST algorithm are made available by NOAA (http://noaasis.noaa.gov/NOAASIS/ml/sst.html), following the launch of the NOAA series of satellites, i.e. NOAA-12, NOAA-14, NOAA-15, NOAA-16, NOAA-17. The output SST data are mapped on desired projection over the ocean area surrounding Japan. Daily composite data are created for every day from several passes over Japan. We use the output SST images from the above image processing systems in binary form as input for the PISCES.

The PISCES can be installed and operated on a standard personal computer with moderate processing power and RAM. The display mode of the monitor should be set to 1024×728 pixels, for imaging of the PISCES generated outputs. The PISCES has basically five functions: 1) generation of multi-pass/multi-date SST composites and averaged images, 2) detection and removal of localized cloudy or non-SST spurious pixels, 3) interpolation at the gappy (cloudy/non-SST) pixels, 4) regeneration of the SST image, and 5) production of SST maps with appropriate geo-position markers and thermal contours. Processing steps for running these functions are shown in a generalized flow chart (Fig. 2). The flow chart shows that the TeraScan generated daily MCSST image is used as the input in the PISCES and a valid daily SST image without cloud cover is produced as the output. Finally the output image is stored in a database, to be eventually used as "reference" or "donor" image while processing the images for the following day(s). Thus all functions of the PISCES work in a loop for regular production of daily SST maps. However, to produce a SST image for a discrete date, the daily images for SST for the previous day or a composite image for the previous days (or week) can be used as "reference" or "donor" image.

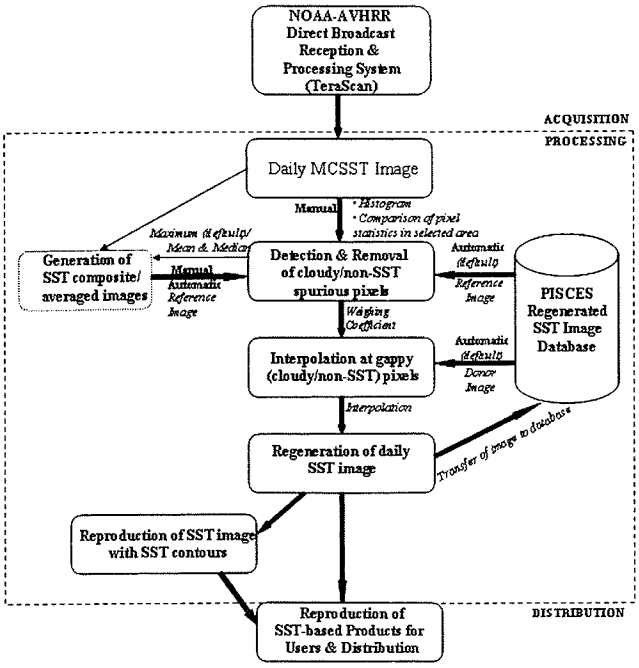

Figure 2. Configuration of the PISCES showing the steps involved in producing the daily SST based products as outputs. The solid arrows represent the operational (default) component and shaded arrows as well as arrows with thin line represent optional user-friendly components available with the PISCES.

In this paper we present all computations using digital numbers (DN) and SST values interchangeably. In the PISCES, DN is converted into an SST value in degree Celsius by the equation: SST (°C)=(DN×0.2)−10.

Description the PISCES functions

Generation of Multi-pass/Multi-date SST Composite and Averaged Images

If cloud free SST images are not available for the duration ranging from a few days to a few weeks, it is often preferred using composite SST image for that duration. The satellite derived SST composites are considered a supplementary tool for acquiring information about SST distribution over a specific area. Conventionally ship observed temperature data recorded at discrete stations over a time period of a few days are used to plot SST contours. The satellite derived SST composites of the duration of a few days are comparable to such conventional products.

In the PISCES the composites are produced using the "maximum" values of the same pixels from a series of images over the desired duration (Fig. 3a and d). Options are available for producing averaged images using both arithmetic mean (Fig. 3b and e) and median (Fig. 3c and f). The PISCES estimates these statistics for each pixel from a se-

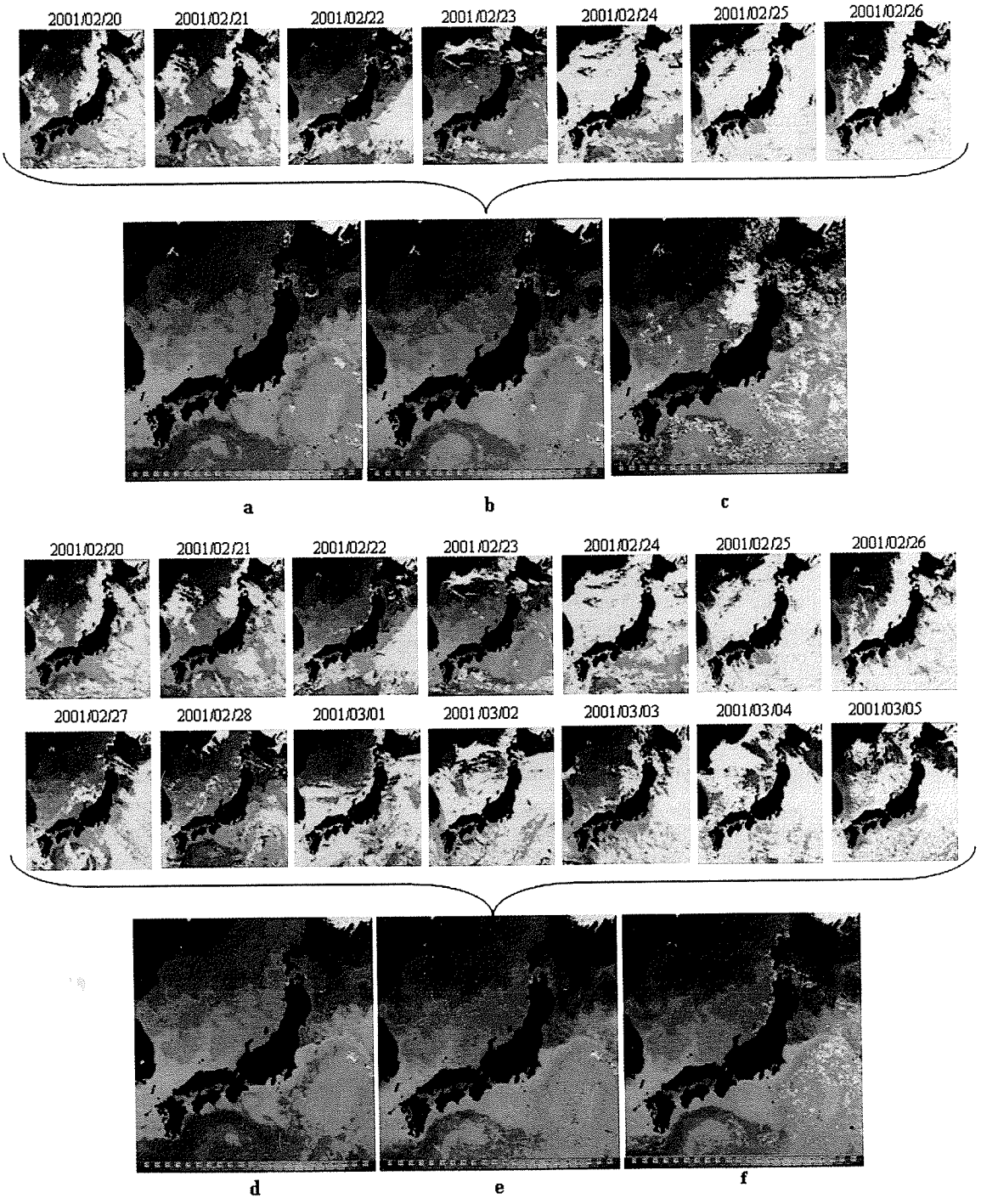

Figure 3. The composite and averaged images produced by using maximum (a and d), arithmetic mean (b and e) and median (c and f) of the pixel values from a series of daily SST images spreading over 1-week (a–c) and 2-weeks (d–f) period. The blue at the left end and red at the right end of the color bars correspond to the lower SST and higher SST. Black and white masks overlays depict the land and cloud areas on the image respectively.

ries of images over the desired duration for generating the averaged images. Spurious pixels are first removed from all input images to ensure inclusion of the pixels with valid SST values in composite making. The function available in the PISCES for removal of spurious non-SST pixel is discussed in the later section of this paper.

Composites and averaged images produced for a short duration (≤one week) are preferred over a longer duration by oceanographers because processing of the former involves less statistical bias, thus with less temporal artifacts. However, the composite and averaged images produce varying level of artifacts for different temporal duration. The SST composites produced over one-week (Fig. 3a) and two-weeks (Fig. 3d) duration using the "maximum" value depict small scale eddies associated with warm streamer off Sanriku, along eastern coast of Japan, more conspicuously in case of the former than the later. However, both the composites show almost no artifacts. The image based on the one-week "median" shows more artifacts (Fig. 3c) compared to that of two-week (Fig. 3f). On the contrary the averaged image based on "arithmetic mean" shows more artifacts on the two-week image (Fig. 3b) than that of one-week (Fig. 3e).

It is worth noting that the PISCES is meant for routine production of SST maps. In the absence of a regenerated valid SST image for the preceding date, the composites are used as "reference" image initially for detection and removal of cloudy and non-SST spurious pixels in the PISCES as described in the next section of this paper. A suitable seasonal window is to be decided upon for generating such composite for effective cloud removal on the "target" images. During seasonal transitions, SST is expected to undergo rapid change even over the duration of a few days. Such transition periods should be avoided while producing a composite SST image especially based on the "maximum" pixel values. So, one should be familiar with the seasonal patterns of SST variability over the given area before generating the composite image.

Detection and removal of localized cloudy and non-SST spurious pixels

The cloud masked SST output images are known to leave areas with ambiguous pixel values, which should be properly detected and removed first by assigning them with the dummy values same as the cloudy pixels, before interpolating SST for the cloud covered areas on an image.

The PISCES has provision to detect these spurious pixels using different methods. It can be performed right away by using histogram of the digital values for a selected area in the image. It is possible to detect the spurious pixels in the sample area due to appearance of a false peak in a flat region of the histogram due to unusually higher digital values (Fig. 4a). The spurious pixels in the sample area can be removed by masking the false peak region. This method can be repeated in other localized sampled area by examining pattern of the histogram of the pixels. Although this method is convenient to detect and remove localized patch of spurious pixels from an image, it needs the users to be judicious in applying the processing techniques. Hence this technique is subjected to possible human error, especially when used by a novice.

There are provisions in the PISCES to detect and remove the spurious pixels from the image after visual interpretation. This process is carried out by using a PISCES-regenerated image of the previous day with estimated SST as "reference" image, for detecting the spurious cloudy pixels on the "target" image. In case the "target" image is a composite, a composite image for the preceding period with one-day time lag devoid of cloudy or spurious pixels is used as the "reference" image (Fig. 4b). Detection of spurious pixels is carried out comparing the spurious pixel value in the "target" image against the minimum pixel value of a selected area on the "reference" image. If the pixel values in the target image are found to be lower than the minimum pixel value in the "reference" image, than such values are detected as non-SST pixel and removed by assigning values specified for cloudy pixels (Fig. 4b). This method is also subjected to human error, even though can be used effectively by an experienced user.

Default provision available with the PISCES for judicious removal of the spurious pixels, constitutes an automatic process. Automatic detection of the non-SST spurious pixels is carried out on the "target" pixel with reference to corresponding pixel in the PISCES-regenerated "reference" image of the previous day. Approximately an 80-km×80-km window (about 20×20 pixels on an image of 512×512 pixels covering seas around Japan) is selected on the "reference" image excluding the "reference pixel" itself. The pixel values less than the variance (s^2) from mean ($\bar{X}$), $<(\bar{X}-s^2)$, of the selected window, are automatically detected as spurious pixel, and hence removed from the target image (Fig. 4c). This method averages SST values of the pixels in close proximity to the "target" pixels of the previous day, and decrease in SST more than the variance after an interval of one day is assumed to be out of possibility under normal ocean condition. The size of the window is based on the well known fact that the Kuroshio Flow moves at a velocity of about 80 km per day, hence the SST values estimated from window size of identical magnitude limits the possibility of estimated SST to be influenced by dynamics of the Kuroshio Flow. This method effectively removes the spurious non-SST pixels and retains the pixels with realistic SST values.

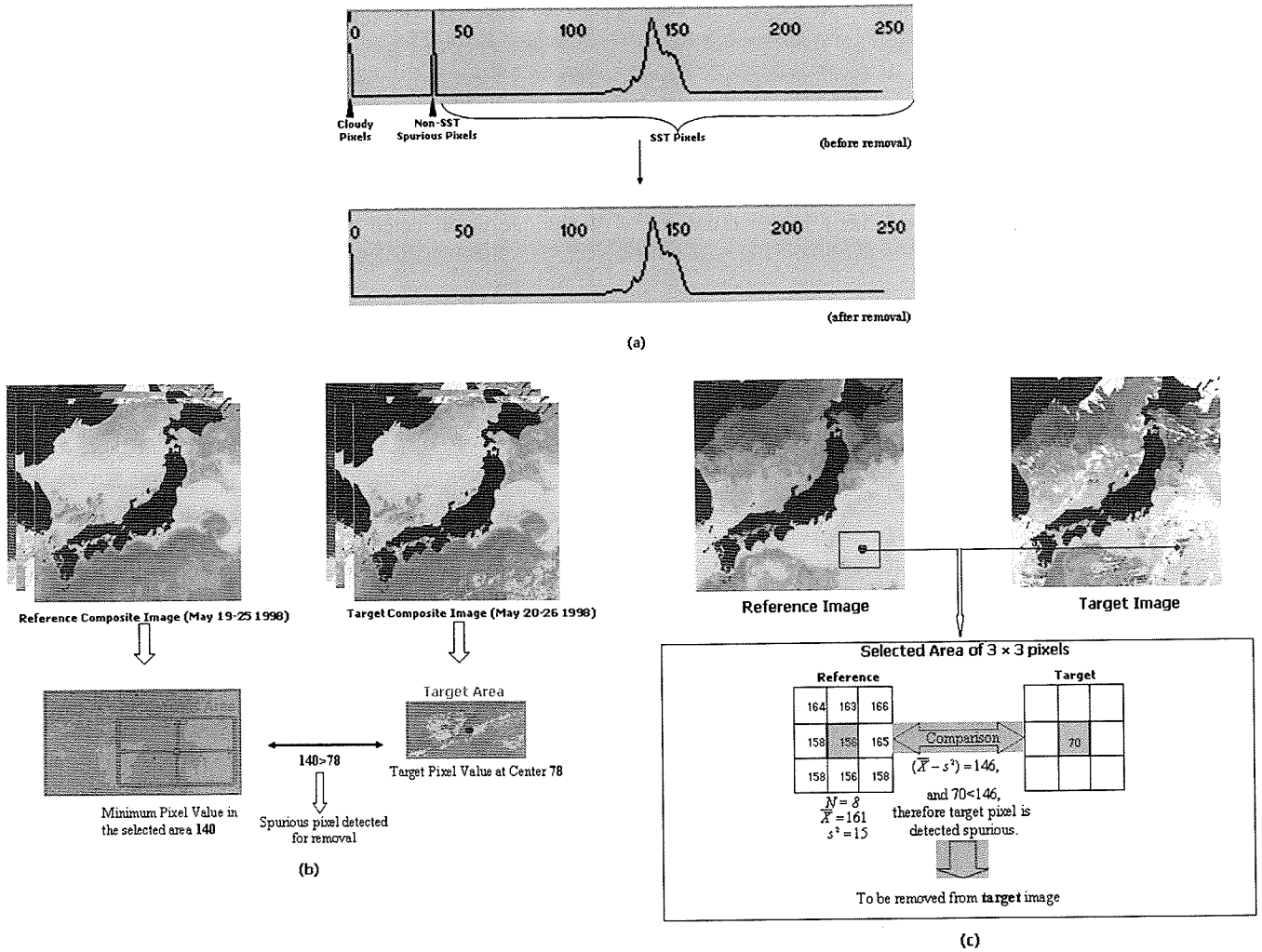

Figure 4. Options available on the PISCES for detection and removal of localized cloudy and non-SST spurious pixels: (a) detection and removal of spurious pixels from a selected area on the image using pixel histogram; (b) comparison of "target" pixel value at the center of a selected area against the minimum pixel value in the corresponding area on the "reference" image of the preceding day(s). If target pixel value is less than minimum pixel value on the "reference" image, than the target pixel is detected as spurious pixel, however, if target pixel value is more than reference minimum pixel value, than the target pixel value is retained as real value; (c) Automatic comparison of "target" pixel value at the center of a selected area against the $(\bar{X}-s^2)$ of the corresponding area on the PISCES-regenerated "reference" image of the previous day keeping the "reference pixel" empty. If target pixel value is less than $(\bar{X}-s^2)$, of the selected area on the "reference" image, than the target pixel is detected as spurious pixel, thus removed from the image. If target pixel value is more than $(\bar{X}-s^2)$ of the selected area on the reference image, than retained as valid SST value.

Interpolation at the gappy pixels and regeneration of the SST image

After successful removal of cloudy and non-SST spurious pixels from the input image, pixel-wise interpolation is carried out at the gappy pixels on the image using a statistical algorithm adopted from numerical method used for analysis of meteorological data (Bergthórsson and Döös, 1955). The SST values estimated by this method at the gappy pixels is obtained as weighed mean of the SST derived from the surrounding pixels by following five steps.

In the first step, a circle is constructed by taking a fixed number of pixels as diameter and keeping the "target" pixel at the center of the circle (Fig. 5a). The circle was used to assess the proximity of all pixels within the circle with reference to the target pixel. Pixels covered partially within the circle are ignored before undertaking interpolation. In the second step the arithmetic mean $(\bar{X})$ and standard deviation (SD) of all cloud-free pixels within the circle is computed to remove the influence of cloudy pixels from the estimation process and the cloud-free pixels with values outside $(\bar{X})\pm$SD are ignored to remove further the influence of widely deviated values from the estimation (Fig.

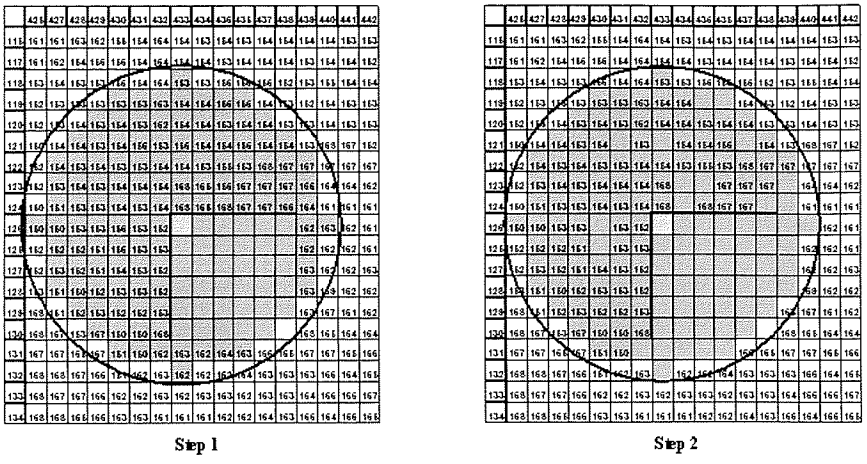

(a)

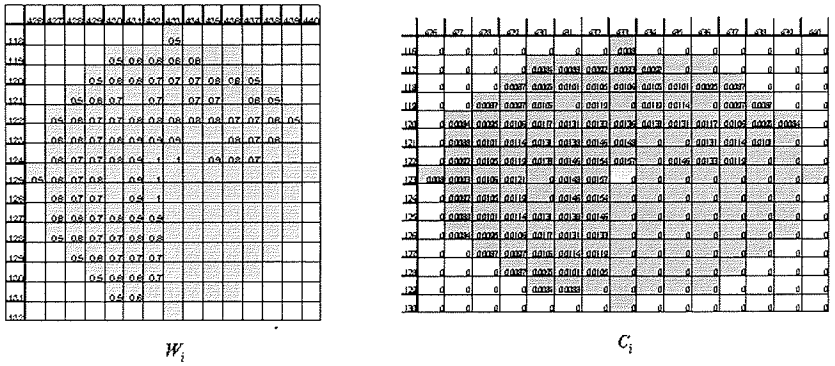

(b)

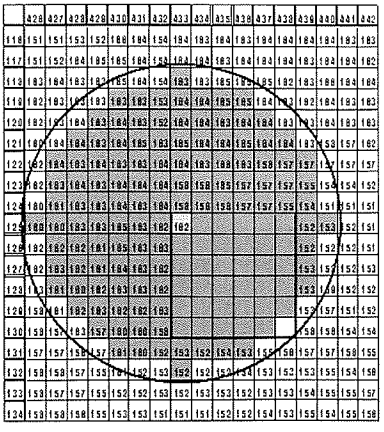

(c)

Figure 5. Steps followed for interpolation of SST at the gappy pixel at the center of the circle with a diameter (please see the text) of 15 pixels: (a) *Step 1*—Initial pixel values within the circle constructed around the "target" pixel, *Step 2*—Pixel values after removing the values outside $(\bar{X})\pm$SD of the initial pixel values; (b) Weighing coefficients, W_i and C_i computed for all pixel locations of the *Step 2* of (a); (c) Estimated pixel value, T_{est} at the "target" pixel.

5a). In the third step, $(\bar{X})$ of the remaining pixels is recalculated and assigned to the cloudy pixel at the center of circle. The mean value, T_{av}, is assumed to be the average of all pixels in the circle with SST values under normal ocean condition and it excludes the ones with extreme values from the interpolation process. In the fourth step, a weighing coefficient C_i is calculated using the following equations to estimate the SST for the target pixel at the center of the circle:

$$C_i = \frac{w_i}{\sum_{i=1}^{n} w_i} \tag{1}$$

and

$$W_i = \frac{1}{1+\left(\frac{R_i}{R_{\max}}\right)^2} \tag{2}$$

C_i and W_i computed for sample image area of Fig. 5a are presented in Fig. 5b. R_i is the location of the every pixel within the circle with reference to the target pixel and $R_{\max}$ is location of farthest pixels with reference to target pixel at the center of the circle. So $R_{\max}$ is radius of the circle expressed as number of pixels. For routine estimation of SST, 8 pixels are used for $R_{\max}$ as default in the PISCES. This value can be changed depending upon the resolution of the target image. Finally the estimated value of the "target" pixel was derived using the weighing coefficient, C_i as follows:

$$T_{est} = T_{av} + \sum_{i=1}^{n} C_i (T_i - T_{av}) \tag{3}$$

where, T_{est} is estimated pixel value (Fig. 5c), T_{av} and T_i are respectively the mean of all pixels within the circle and the values of individual pixels, under the normal ocean condition.

Regeneration of the SST Images

In case of small patch of gappy pixels, the above method can be used successfully for interpolation, to produce a cloud free image. However, in case of an image with extensive cloud cover for a specific day, the PISCES makes it the "recipient" image, and the cloud free image regenerated for the previous day becomes the "donor" image. Pixel values from the "donor" image is used for filling up the cloudy pixels in the "recipient image" by keeping two pixels as blank around the edge of the filled up area (Fig. 6a–c). The blank pixels are later filled up by the interpolation technique as discussed before, using the weighing coefficients as derived from (1), (2) and (3). As a result, an output daily image devoid of cloudy pixels is generated for the "target" day. However, It is worth noting that the values in the filled up areas of the resultant image represent the SST values of the "donor" image (of previous day). Therefore the PISCES re-estimates the SST values in the filled up area, using the following three steps: 1) line of two blank pixels were created along the inner edge of already interpolated pixels within the "donated area", 2) these blank pixels are filled up by the estimated values using same interpolation technique as followed previously using the weighing coefficients as derived from (1), (2) and (3), 3) the estimation process is repeated in centripetal direction (from the outer edge towards the center of the filled up area) creating line of blank pixels adjacent to the just interpolated pixels, until the entire "donated area" are estimated back.

For validation of this technique, a selected area of cloud free pixels on a daily image (May 31 2000) was assigned with the dummy values same as cloud. Entire

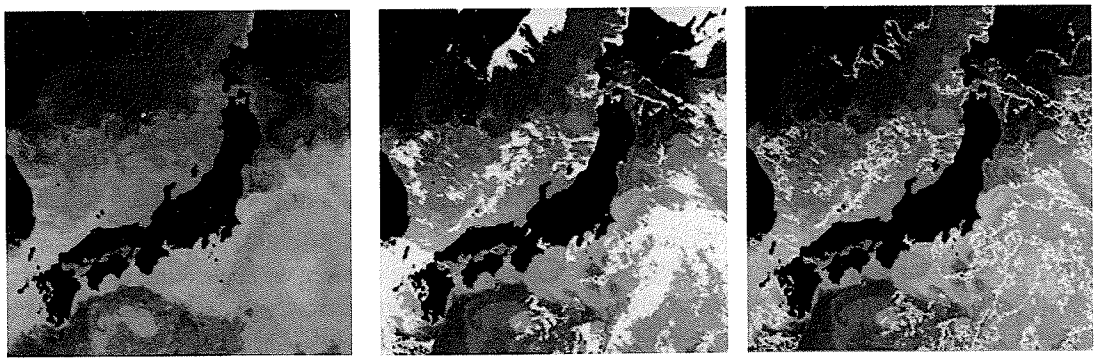

Figure 6. Interpolation of SST on the image with extensive cloud cover: (a) the PISCES generated "donor" SST image for the previous day of the date of "target" image; (b) the "target" image with extensive coverage of gappy pixels which are to be filled up through interpolation by the corresponding pixel values from the "donor" image; (c) the "target" or "recipient" image after filling up the gappy pixels by transferring the pixel values from the "donor" image leaving 2-pixels blank around the edge of the filled up area.

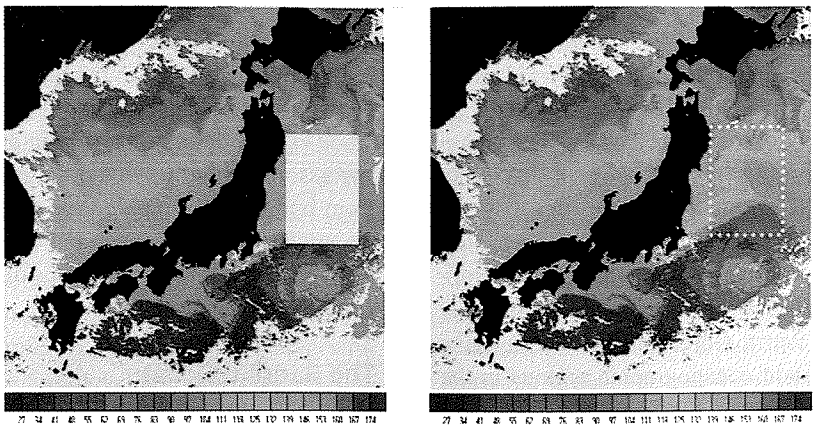

(a) (b)

Figure 7. Validation of the interpolation method available with the PISCES: (a) selected cloud-free area on the SST image of May 31 2000 assigned dummy values same as cloud (white); (b) the selected area after regeneration of SST using default interpolation method of the PISCES. Regenerated SST image of May 30 2000 was used as the "donor" image as described in the section *3.4*.

Table 1. Regression statistics for the comparison between real time SST from a selected area on a daily image (May 31 2000) and regenerated SST using the interpolation and regeneration functions of the PISCES on the daily regenerated image of May 30 2000, where m is the slope and b is the intercept.

Number of Blank Pixels	N	R^2	m	b
2	11570	0.999	0.9997	0.0034
4	11570	0.995	0.9971	0.0458
6	11570	0.990	0.9976	0.0141
8	11570	0.985	0.9993	−0.0428

process of interpolation and re-estimation as cited above, was carried out to regenerate the selected area from the PISCES by taking the PISCES regenerated image of 30th May, 2000 as the "donor image" (Fig. 7). Re-estimation was carried out by creating 2, 4, 6 and 8 blank pixels at the outer edge while filling the blank area and along the subsequent inner edges while estimating back the area in the centripetal direction. The regenerated values were subsequently regressed against the real image values and results are presented in the Table 1. Significant relationship was noticed from this regression underlining the effectiveness of our statistical method to remove temporal artifacts from the interpolated image (Fig. 8). However, regression coefficient (R^2) was noticed to be highest with 2-pixel blanks and reducing with the increase in number of blank pixels (Table 1). Such result indicates that one-blank pixels would provide the best re-estimated values, however it would require enormously long time to carry out such processing on an

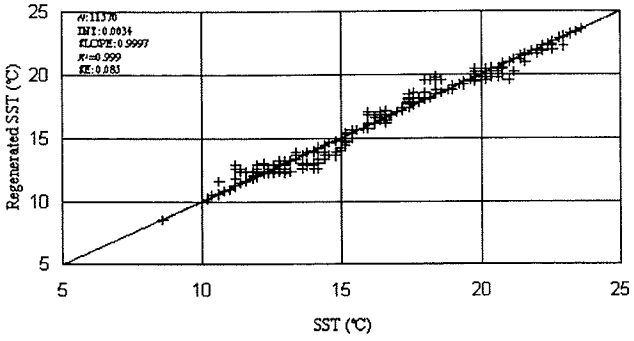

Figure 8. Comparisons of the real time SST from the image of May 31 2000 and regenerated SST using the PISCES regenerated SST image of May 30 2000 using the estimation technique as described in the section *3.4* and shown in Fig. 7.

image of 512×512 dimension using a common PC. Therefor 2-pixel blank was considered best compromise for using as default in the PISCES.

Generation of SST contour map

The PISCES has option to generate contours on a SST image at different temperature intervals. This function was added to the software by using an in-house computer program, based on Discrete Fourier Transform (DFT) model. This function enables the user to generate smoothened thermal contours at specified ranges and to identify the localized thermal features such as eddies. Some outputs using this function are presented in the next section of this paper. Details of the contouring function are not presented since it is out of the scope of this paper.

Sample outputs from the PISCES

In this section, we present The PISCES-generated sample outputs (image and SST contours) for two selected areas near the Sanriku Coast and the Boso East Coast near Japan as case studies. The Sanriku Area described in this section extends from 37.5°N to 42.4°N and from 139.8°E to 146.2°E comprising the Kuroshio Extension, the Tsugaru Warm Current and the Oyashio. Warm water spreading from the Kuroshio, cold water spreading from the Oyashio, existence of several small and meso-scale eddies and formation of the Kuroshio Warm Core Ring (KWCR) make the area one of the important oceanographic regions in the northern Pacific Ocean. Moreover, the Sanriku Area is considered to be one of the major pelagic fishery ground. On the other hand the area near the Boso East Coast represents an area from 30.8°N to 36.1°N and from 135.3°E to 141.7°E comprising three major bays (Suruga Bay, Segami Bay, Tokyo Bay) opening to the sea on the southern coast of Honshu, Japan. In this area several small islands such as Oshima, Niijima, Kozushima and Miyakejima are located. The Kuroshio flows through the area, off the bay mouths with varying strength, and on temporally variable path. The current in the bays along the Boso East Coast, are influenced by variations in the path and strength of the Kuroshio. Moreover, wind induced upwelling is prevalent in this area especially in the lee of the islands and along the Kuroshio front. The bays and the Kuroshio front in this area are also considered to be fishing ground for various pelagic species. Considering the importance of these two areas from both oceanographic process and fishery point of view we undertook the case studies to assess utility of the PISCES outputs to infer various oceanographic features relevant to fishery ground.

The Sanriku Coast:

Daily SST images for the month of October 1999 covering the area near the Sanriku Coast between the warm Kuroshio Extension and the cold Oyashio Front were produced using the default functions of the PISCES (Fig. 9) to depict temporal changes of some important thermal features such as warm streamer, cold streamer and the KWCR in this dynamic ocean area. These images show the Kuroshio Extension at the southeast part of the image area characterized by distinctly high SST. The warm streamer was noticed leading to the north from the south. The KWCR was found rotating clockwise southeast of the Hokkaido. These images

Figure 9. Time series daily SST images of the Sanriku Area, east of Japan during October 1–30 1999 produced as outputs from the PISCES using the default functions.

(Fig. 9) depict structural change of the KWCR as well as temporal changes in the location of the warm streamer and the Oyashio Intrusion over a period of one month during the fall. Furthermore, SST images and SST related products of the same area during 29th September–2nd October 1999, (Fig. 10–13) are presented to underline the utility of the PISCES outputs to detect mesoscale thermal features over a short duration. The PISCES regenerated SST images of the Sanriku Area (Fig. 11) were produced using daily SST images as input (Fig. 10) and the PISCES regenerated image of the previous days as "reference" and "donor" images respectively for spurious pixel removal and SST interpolation at cloud masked pixels.

A number of dark blue spots can be marked in the cloud-masked area on the daily SST images of the Tohoku Area (Fig. 10). These spots can be attributed to the spurious pixels as described earlier. Such localized ambiguous pixels were removed and SST interpolation was carried out subsequently by using the default options available with the PISCES. Major mesoscale thermal features associated with the "perturbed area" (Kawai, 1972) between the warm Kuroshio Extension and the cold Oyashio Front can be distinctly marked from the output SST images (Fig. 11) and the SST contours (Fig. 12). The Kuroshio Extension can be marked at the southeastern part of the images and the warm streamer leading to the north from the south. The KWCR can be noticed rotating clockwise southeast of Hokkaido. Intrusion of cold Oyashio waters to the center of the KWCR can be attributed to clockwise rotation of the warm eddy. These conspicuous thermal features are linked to vortex motion induced by the meandering flow patterns widely known as first and second Oyashio Intrusions (Kawai, 1972). These thermal features are distinctly depicted in satellite SST thermal contours generated using the PISCES (Fig. 12). However, the SST contour map plotted using ship based oceanographic observation of the Hakodate Marine Observatory, in the seas south of Hokkaido and east of Honshu during September to October 1999 (Fig. 13a) fails to depict these features due to limited oceanographic observation points used for plotting the contours. The ship SST contours provide only broad idea about the extent of the Kuroshio Extension and the Oyashio Front. The SST con-

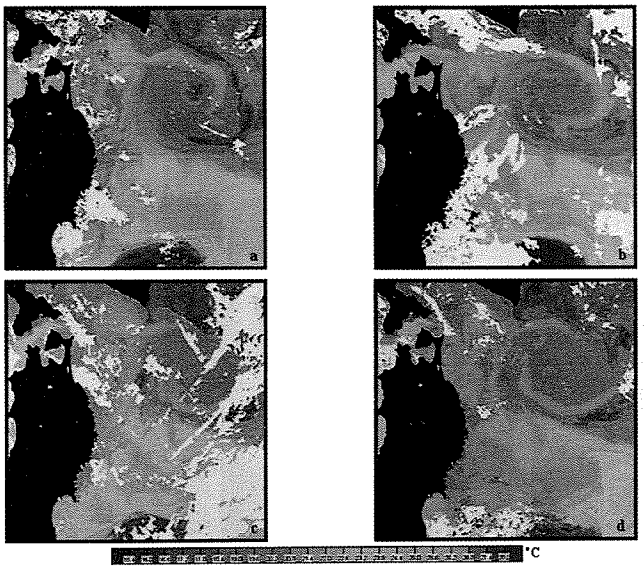

Figure 10. Daily SST images of the Sanriku Area during September 29–October 02 1999 used as the input on the PISCES. (a) September 29 1999 (b) September 30 1999 (c) October 01 1999 (d) October 02 1999.

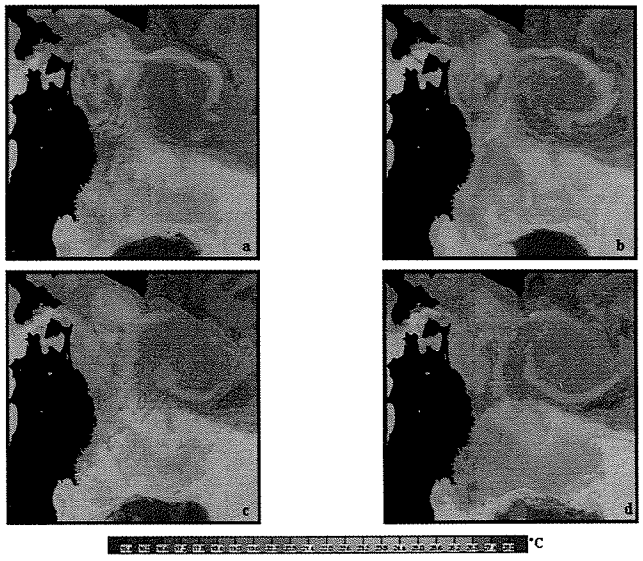

Figure 11. Daily SST images produced as outputs from the PISCES for the same area and same dates as presented in Fig. 10.

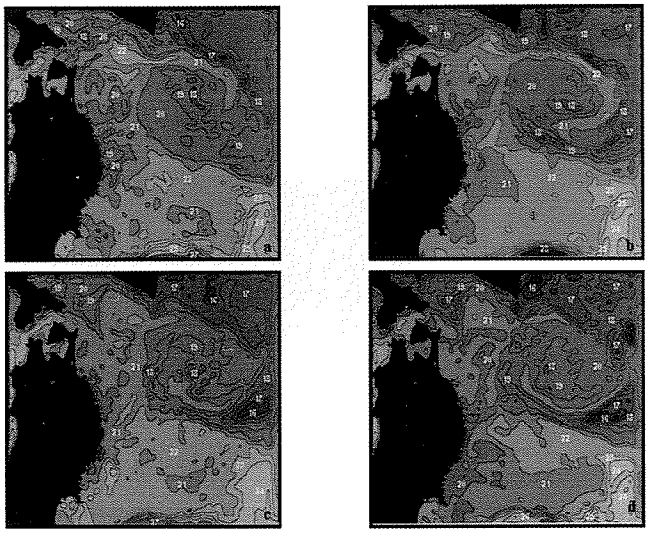

Figure 12. Daily SST contours produced from the PISCES for the same area and same dates as presented in Fig. 10.

tour map as presented in Fig. 13b was reproduced from the Quick Reports on the fishing and oceanographic conditions published by the JAFIC. This contour map is based on the ship observed SST routinely provided by the fishing vessels to the JAFIC and satellite derived SST data. Thus, all important sea surface thermal features as discussed earlier can be noticed from this contour map. This map further shows the fishing ground for different pelagic fishes such as skipjack, flying squid and saury (Fig. 13b). It can be noted that such fishing grounds were mostly located in the frontal regions. Skipjack fishing grounds (shaded polygons) were noticed moving anticyclonically along the warm streamer around the KWCR during September–October and the fishing ground was formed in the Kuroshio fronts with SST range of 22–23°C (Sugimoto and Tameishi, 1992). Likewise Saitoh *et al.*, (1986) reported the Pacific saury coming down from the north along the cold streamer associated with the Oyashio flow. Fishing grounds for flying squids were also reported in the waters around the KWCR, with the close proximity to the coast (Sugimoto and Tameishi, 1992). Delineation of the fishing grounds in the Fig. 13b was based on such reported information. The SST contours as derived from the PISCES generated outputs (Fig. 12) are capable of providing such information for delineation of the fishing grounds.

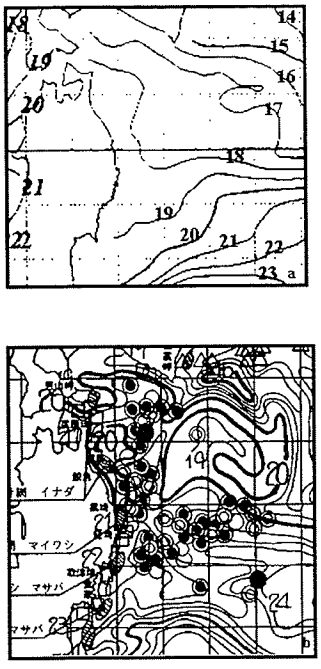

Figure 13. The SST contour maps produced by Japanese agencies based on the oceanographic observation in the seas south of Hokkaido and east of Honshu during September to October 1999. (a) Monthly mean SST in October (°C) from Oceanographic Observation Report of the Hakodate Marine Observatory (b) Schematic map of the oceanographic conditions from the Quick Report of the JAFIC for October 06 1999 showing different pelagic fishing grounds as marked by open and solid circles, and shaded polygons.

The Boso East Coast

The SST products for another area, the Boso East Coast, along the southern Japanese coast of Honshu during 26–28th April, 1999 are presented in Fig. 14–17. The PISCES regenerated SST images of the southern Japanese coast of Honshu (Fig. 15) were produced using daily SST images as input (Fig. 14) and the regenerated image of the previous days as the "reference" and the "donor" images. The SST contours based on the ship measured SST for the corresponding periods, produced by two Japanese agencies (JAFIC and the Kanagawa Prefectural Experimental Fishery Station), are presented in Fig. 17 for comparison with the satellite SST thermal contours (Fig. 16) to highlight utility of the PISCES in providing user-friendly and application oriented ocean information.

The PISCES generated SST images of 27th and 28th April, 1999 (Fig. 15) provided SST distribution pattern in the sea along the southern Japanese coast of Honshu , the Boso East Coast, using the daily SST images as input (Fig. 14). The SST contour map as presented in Fig. 17a was re-

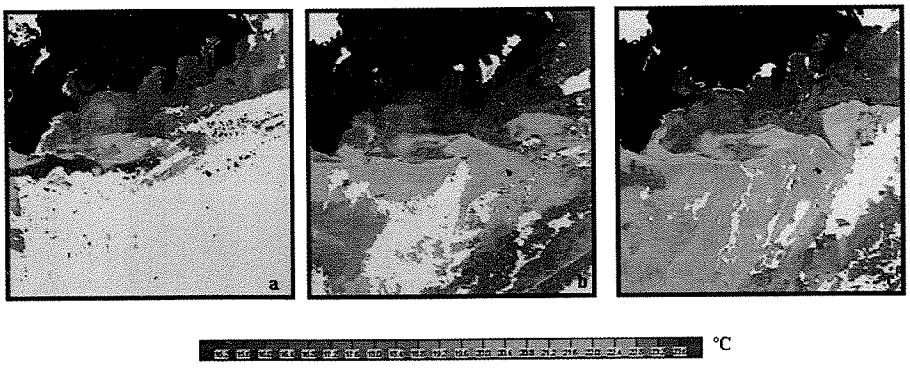

Figure 14. Daily SST images off the southern Japanese coast of Honshu (the Boso East Coast) during April 27–29 1999 used as the input on the PISCES: (a) April 27 1999; (b) April 28 1999; (c) April 29 1999.

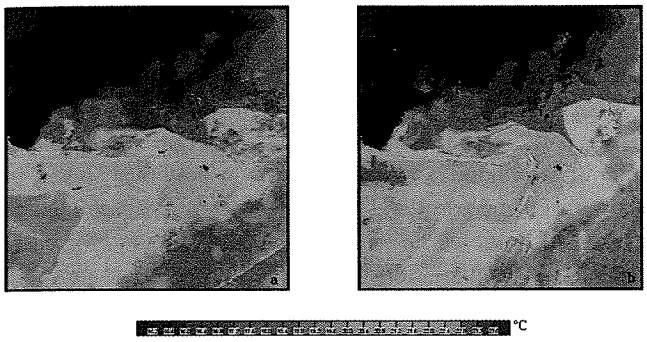

Figure 15. Daily SST images produced as outputs from the PISCES for the same area as presented in Fig. 14 on April 28 1999 and April 29 1999.

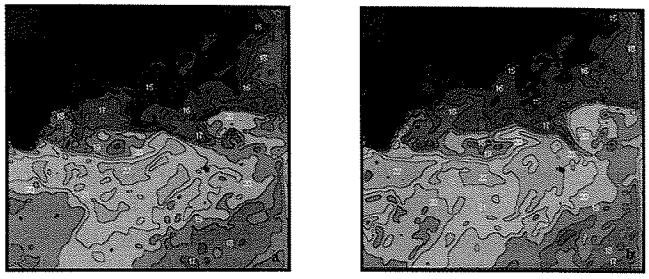

Figure 16. Daily SST contours produced from the PISCES for the same area as presented in Fig. 14 and same dates as presented in Fig. 15.

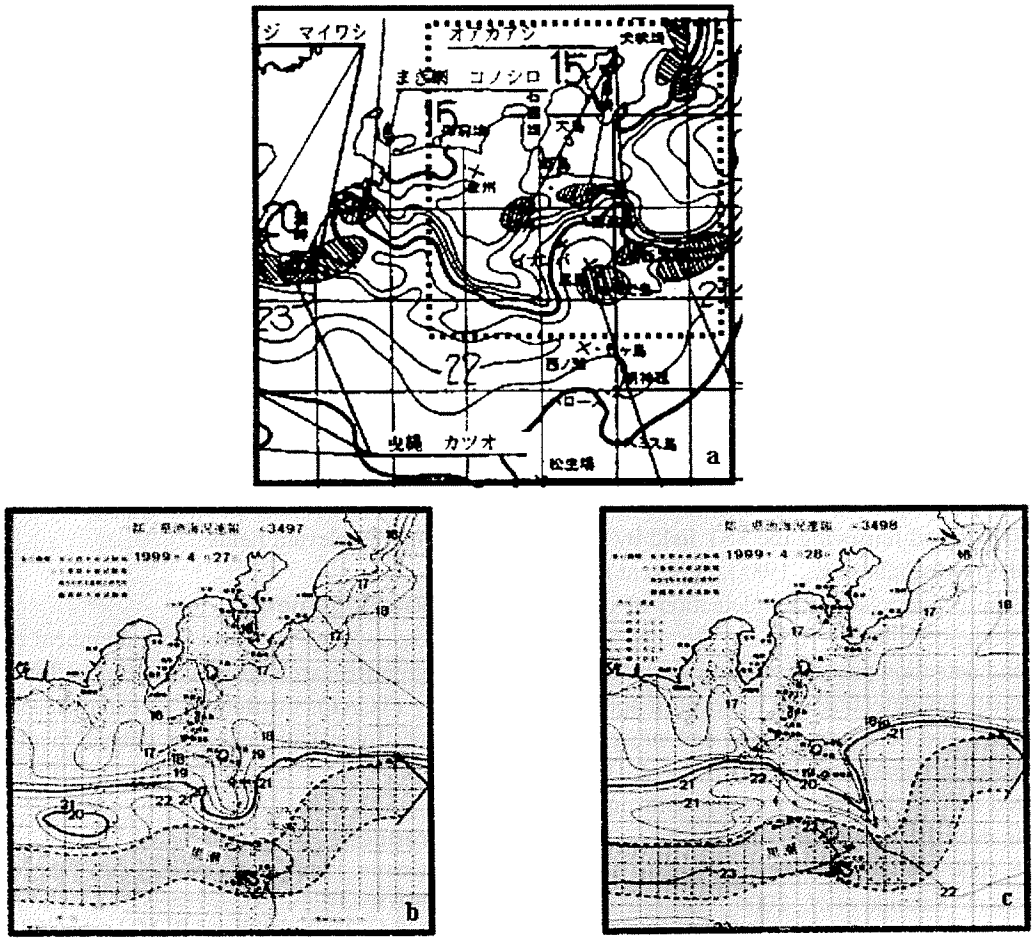

Figure 17. The SST contour maps produced by Japanese agencies based on the oceanographic observation off the southern Japanese coast of Honshu (the Boso East Coast) during April 27–28 1999: (a) Schematic map showing the oceanographic conditions from the Quick Report of the JAFIC during April 27–28 1999 showing the skipjack fishing grounds (polygons with dotted line); (b)–(c) SST contours (°C) on April 27 and April 28 1999 as published by the Kanagawa Prefectural Experimental Fishery Stations.

produced from the Quick Reports on the fishing ground and oceanographic conditions published by the JAFIC for the same period. The skipjack fishing grounds (shaded polygons) as shown along the Kuroshio flow (Fig. 17a), were located based on the information on frontal areas. Such thermal fronts can be well deciphered from the PISCES generated outputs, thus such outputs were found useful in generating fishing ground information. Furthermore, the SST contours (Fig. 16) were found in good agreement with the contour maps produced by the Kanagawa Prefectural Experimental Fishery Stations based on the ship observed SST data (Fig. 17b–c). Especially the meandering pattern of the Kuroshio Flow south off the bays can be noticed to follow identical trend in both the products even though they are based on data from different sources. Agreement between the features detected from satellite derived SST field and thermal contours published by the Kanagawa Prefectural Experimental Fishery Stations (http://www.agri.pref.kanagawa.jp/SUISOKEN/kaikyozu/1to3ken.asp) underlines relevance of the PISCES generated products to provide useful information about the oceanographic condition in the ocean especially related to pelagic fishery ground.

Summary and Conclusions

This paper presents the PC-based PISCES system developed to produce user-friendly high spatial resolution SST products in seas around Japan. The TeraScan System of the SeaSpace (http://www.seaspace.com/main/product_line/hrpt/hrpt.html) and the Advanced-HIGHERS (A-HIGHERS) developed by Sakaida *et al.* (2000), respectively based on the workstation and the super computer, are presently being used in Japan for receiving the HRPT data from NOAA-AVHRR and retrieving the SST field by using the MCSST method (McClain *et al.*, 1985). Different methods are used in these two systems for detection of cloud. Based on our experience with the TeraScan System, we noticed that the cloud detection process available with the system to be inadequate for detecting and removal of spurious pixels. Despite the cloud detection process and subsequent quality control (QC) process available with the A-HIGHERS was reported to be effective in dealing with most of the cloudy pixels over the image area, possibilities of misjudgment in the clear-cloudy classification seems to still exist with the system (Sakaida *et al.*, 2000). Despite its advanced cloud detection process, the A-HIGHERS is beyond the reach of the most of the potential users since it is a super-computer based in-house system. On the contrary the TeraScan is commercially distributed system and presently being used by several institutes and organizations in Japan for receiving and processing HRPT data of NOAA-AVHRR. The PISCES was designed to use the output SST image from any image processing system in the binary format, as input. The system can be conveniently used as the QC component for efficient detection and removal of such spurious pixels from the input SST images. The PISCES also carries out the SST interpolation at cloudy pixels and continuous regeneration of daily SST images by adopting judicious statistical methods previously used in the field of meteorology. As evident from the case studies presented in the earlier section, the PISCES can efficiently deal with SST variations in the "perturbed area" near the Sanriku Coast where the ocean surface features (Kuroshio Extension, Warm Core Rings *etc.*) undergo significant structural and temporal changes over short time interval. Such areas of frontal activity and strong thermal gradients are considered more difficult for regeneration of SST through interpolation compared to the area with less frontal activities and weak thermal gradients. Since the software can be used efficiently in former case it is expected to perform well in the later case as well. However, there are scopes for further improvement with the functions of the PISCES to produce more accurate SST fields in diverse ocean areas.

The PISCES is basically aimed at routine production of user-friendly daily SST maps from high resolution satellite imagery for the potential users especially in the fishery sector. Our sample studies demonstrate effectiveness of the system in dealing with problems inherent with the SST images generated by Japanese organizations using existing image processing systems, especially in retrieving necessary thermal features for identification of pelagic fishing grounds. In order to make our system more user friendly, we will continue our efforts to improvise the output products in future versions through active consultation with users in the relevant fields.

Acknowledgements

We acknowledge supports from members of the Ocean Information Research Team at the Center for Advanced Technology (TCAT), Institute of Oceanic Research and Development, Tokai University for development of the PISCES System.

References

Bergthórsson, P. and B. R. Döös (1955) Numerical weather map analysis. Tellus, **VII**, 329–340.

Fiedler, P. C., G. B. Smith and R. M. Laurs (1985) Fisheries applications of satellite data in the eastern North Pacific. Mar. Fish. Rev., **46**, 1–13.

Fiúza, A. F. G. (1990) Application of satellite remote sensing to fisheries. In. Operations Research and Management in Fishing, ed. A.G. Rodrigues, Kluwer Academic Publishers, Dordrecht, the Netherlands, 257–269.

Gower, J. F. R. (1982) General overview of the nature and use of satellite remote sensing data for fisheries applications. NAFO Science Council Studies, **4**, 7–19.

Hirai, M. (1985) On an application of infrared remote sensing techniques to the fisheries oceanography-analysis of the fine structure in saury fishing grounds using infrared images obtained from NOAA-6 satellite. Sora to Umi, **7**, 1–10.

Kawai, H. (1972) Hydrography of the Kuroshio Extension, In. Kuroshio: Its Physical Aspects. eds. H. Stommel and K. Yoshida, University of Tokyo Press, 235–352.

Laurs, R. M. and J. T. Brucks (1985) Living marine resources applications. Adv. in Geophys., **27**, 419–452.

McClain, E. P., W. G. Pichel and C. C. Walton (1985) Comparative performance of AVHRR-based multi-channel sea surface temperatures. J. Geophys. Res., **90**, 11587–11601.

Montgomery, D. R. (1981) Commercial applications of satellite oceanography. Oceanus, **24**, 56–65.

Saitoh, S., S. Kosaka and J. Iisaka (1986) Satellite infrared observations of Kuroshio warm-core rings and their application to study Pacific saury migration. Deep-Sea Res., **33**, 1601–1615.

Sakaida, F., J. Kudoh and H. Kawamura (2000) A-HIGHERS-the system to produce the high spatial resolution sea surface temperature maps of the Western North Pacific using the AVHRR/NOAA. J.Oceanogr., **56**, 707–716.

Sugimoto, T. and H. Tameishi (1992) Warm-core rings, streamers and their role on the fishing ground formation around Japan. Deep-Sea Res., **39**, 183–201.

Walton, C. C. (1988) Nonlinear multichannel algorithms for estimating sea surface temperature with AVHRR satellite data. J. Appl. Meteorol., **27**, 115–124.

Walton, C. C., W. D. Pichel, J. F. Sapper and D. A. May (1998) The development and operational application of nonlinear algorithms for the measurement of sea surface temperatures with the NOAA polar-orbiting environmental satellites. J. Geophys. Res. **103**, No. C12, 27999–28012.

Yamanaka, I. (1982) Application of Satellite Oceanography to fisheries studies in Japan. NAFO Science Council Studies, **4**, 41–50.

日本周辺における高解像度衛星データを使用した海表面水温図簡易PCソフトウェア—PISCESの開発

岡田喜裕[†1,3]，森脇　亮[2]，ケダーナッシュ・マハパトラ[3]

アメリカ海洋大気局のNOAA衛星シリーズに搭載された高解像度放射計 (AVHRR) より得られるデータを使用し，日本周辺の海表面水温 (SST) 情報をユーザーに提供するために，SSTの継続的な推定をパソコン上で簡単に行えるソフト (PISCES) を開発した．そのシステムは，雲などによるノイズピクセルの除去を目的とし，自動的にコンピュータにより海洋の動的過程の考えを導入した統計的な補間手法を使用し，継続的なSST画像の再生を可能にした．本論文では，PISCESシステムの構成と，その各構成要素に用いられる統計学的アルゴリズムについて解説する．

PISCES補間されたソフトウェアからの出力画像は，同日の実在のSSTと比較した結果，良い一致を示した (R^2=0.999)．また，局在的や中規模の海洋現象において海表面水温の特徴を表現する性能を計るために，東海と三陸エリアのケーススタディーによって検証した．その結果，沿岸域では局在的に短期間に変動する渦を表現しきれない制限はあるが，主な海洋現象を調査する際に非常に役立つことが分かった．さらに，漁業者のニーズに応える可能性があると分かった．

[1] 東海大学海洋学部
[2] 株式会社アース・ウェザー
[3] 東海大学フロンティアリサーチセンター
[†] okada@scc.u-tokai.ac.jp